Interference Suppression in Synthesized SAR Images

Andreas Reigber, *Member, IEEE,* and Laurent Ferro-Famil, *Member, IEEE*

***Abstract*—Radio interferences are becoming more and more an important source for image degradation in synthetic aperture radar (SAR) imaging. Especially at longer wavelengths, interferences are often very strong, and their suppression is required during data processing. However, at shorter wavelengths, interferences are often not obvious in the image amplitude, and filtering is not performed in an operational way. Nevertheless, interferences might significantly degrade the image phase, and the estimation of sensitive parameters like interferometric coherence or polarimetric descriptors becomes imprecise. Interference suppression is usually performed on the raw data, which are in most cases not available to the end-user. In this letter, a new interference suppression method for focused SAR images is proposed. Its performance is tested on interferometric repeat-pass data acquired by the German Aerospace Agency's experimental SAR system (E-SAR) at L-band.**

***Index Terms*—Interferometry, radio interferences, radio-frequency interference (RFI) filtering, synthetic aperture radar (SAR).**

I. Introduction

THE MICROWAVE region of the electromagnetic spectrum is becoming more and more used for various civilian (e.g., telecommunication, airport control, etc.) and military purposes. For synthetic aperture radar (SAR) imaging, this is a severe problem, as received radar signals are often corrupted by interferences, caused by external sources of radiation. Modern SAR applications require very high image quality in amplitude and phase; consequently, a precise filtering of radio-frequency (RF) interferences is essential. In particular, the interferometric phase and coherence or polarimetric descriptors like the scattering entropy react very sensitively to phase errors caused by RF interferences.

Nevertheless, up to now, operational RF interference filtering is still uncommon at L-band and shorter wavelengths. At such wavelengths, the effects of RF interferences on the amplitude information are in most cases not obvious. RF interference filtering is not carried out in these cases because it would slightly degrade the sensor's impulse response and, consequently, the overall image quality. Although this might be correct when dealing with amplitude images only, it is important to note that the influence of RF interferences on the interferometric phase and coherence can be much stronger than the degradation, due to a slightly disturbed impulse response.

Usually, radio-frequency interference (RFI) filtering is performed before image synthesis, directly on the radar raw data. Several robust filtering algorithms are described in the literature, mainly based on coherent estimation and subtraction of interfering signals [1] or notch-filtering of the interferences in the range spectral domain [2], [3]. However, in most cases, the raw data are not available to the end-user, who is dependent on proper preparation of the SAR image product by the respective data facility: as explained in detail in Section II, common filtering methods cannot be applied to synthesized SAR data.

This letter proposes a modified RFI filtering approach, adapted to already focused single-look complex SAR images. It has the advantage that focused images can be corrected *in case* disturbing influences of RF interferences are encountered during data analysis. Section II gives an overview of the characteristics of RF interferences, which are used in Section III to design a filtering approach for synthesized SAR images. In Section IV, results based on interferometric L-band data of the German Aerospace Agency's (DLR) experimental SAR system (E-SAR) are presented.

II. Characteristics of RF Interferences

RF interferences have their origin in individual sources of radiation, which can be located far outside of the image swath. In general, RF interferences may have almost every possible spectral characteristics, depending on the respective interfering source (jamming, etc.). Important parameters of RFIs in the context of SAR are, in particular, their bandwidth in the range spectra, as well as their temporal behavior during data acquisition in azimuth. In case of E-SAR, almost exclusively RFIs with a very narrow bandwidth compared to the one of the radar are encountered [3]. Additionally, the influence of interferences is not distributed uniformly in azimuth; in E-SAR, raw-data artefacts typically appear only in some isolated range lines [1]. Interference signals seem also to have particular polarization characteristics: at P-band, the vertical reception channel is typically much more affected by RFI than the horizontal one, while at L-band, most interferences seem to be horizontally polarized. However, it is important to note that RFI characteristics depend strongly on the sensor parameters as well as the geographical region of data acquisition.

In case of SAR raw data, RF interferences appear well localized in the azimuth-time range-frequency domain. This is due to their narrow bandwidth as well as their short duration. In focused SAR images, strong interferences appear as bright wide stripes in the range direction, superimposed upon the SAR image. Weaker ones might not be apparent in the amplitude

Manuscript received July 12, 2004; revised September 19, 2004. This work was supported in part by the German Academic Exchange Service PROCOPE under Project D/0333612 and in part by the French International Cooperation Service under Project 07632TM.

A. Reigber is with the Department of Computer Vision and Remote Sensing, Technical University of Berlin, D-10587 Berlin, Germany (e-mail: anderl@cs.tu-berlin.de).

L. Ferro-Famil is with the Institut d'Electronique et de Téléommunications de Rennes, University of Rennes 1, F-35042 Rennes, France (e-mail: laurent.ferro-famil@univ-rennes1.fr).

Digital Object Identifier 10.1109/LGRS.2004.838419

image, but still have strong influence, for example, on the interferometric coherence.

Simplifying, SAR image formation may be considered as convolution of the SAR signal with a matched filter kernel in both range and azimuth direction in order to transform the raw data into a high-resolution image result. None of the operations affect the narrow bandwidth of the interferences. However, the matched filter in azimuth is adapted to the SAR imaging geometry and not to the interferences. Whereas it focuses the distributed SAR response in the raw data according to its Doppler phase history, it will defocus the interferences, whose characteristics are totally independent of the SAR measurement. Consequently, in synthesized SAR images, interferences appear smeared in azimuth by the length of the reference function in azimuth. Effectively, RF filtering cannot be performed at this stage, as the interference energy is not localized.

In Fig. 1(b), an example of a airborne L-band SAR scene, transformed into the range-frequency azimuth-time domain, is shown. It is affected by interferences, which are visible as small curved features. The curvature is a result of additional processing steps performed during data focusing (range-cell-migration correction, motion compensation, etc.) with a wavenumber domain SAR processor [4].

III. Filtering Algorithm

The principle of the proposed RFI filter is to improve the localization of the interferences before the actual filtering operation by convolving the synthesized image with the inverse of the matched filter function used for azimuth compression. Such an operation defocuses the image content, but at the same time it focuses the interference energy onto the azimuth position it had in the raw data.

However, in general, SAR azimuth processing cannot be simplified to a direct convolution of the raw data with a one-dimensional reference function in azimuth. Additional steps, like range-cell-migration correction are necessary to achieve high image quality. Modern SAR processing algorithms, like chirp-scaling or wavenumber domain processing [4]–[6], distort the initially point-like shape of RF interferences in the range-frequency azimuth-time domain in a two-dimensional way. As can be seen in Fig. 1(b), this causes interference locations following a nonlinear curve in the processed image. To correctly focus the RF interferences, it would, in principle, be necessary to revert all theses effects. In practice, however, the differences are in most cases minimal.

For synthesized SAR images, the processing algorithm and the precise reference function used for azimuth compression often remain unknown. In this case, the theoretical one-dimensional reference function can be used for azimuth decompression. In the range-time azimuth-frequency domain it may be expressed as

$$\Phi(r, f_D) = r \cdot \left(\sqrt{\left(\frac{4\pi f_0}{c}\right)^2 - \left(\frac{2\pi f_D}{v}\right)^2} - \frac{4\pi f_0}{c} \right) \quad (1)$$

with r denoting the range distance, c the speed of light, f_0 the radar center frequency, f_D the Doppler frequency, and v the forward velocity of the sensor [6]. If the sampling of the azimuth spectra is ambiguous due to a high Doppler centroid, precise knowledge of the Doppler centroid variations over range are necessary to correctly calculate f_D for every range distance.

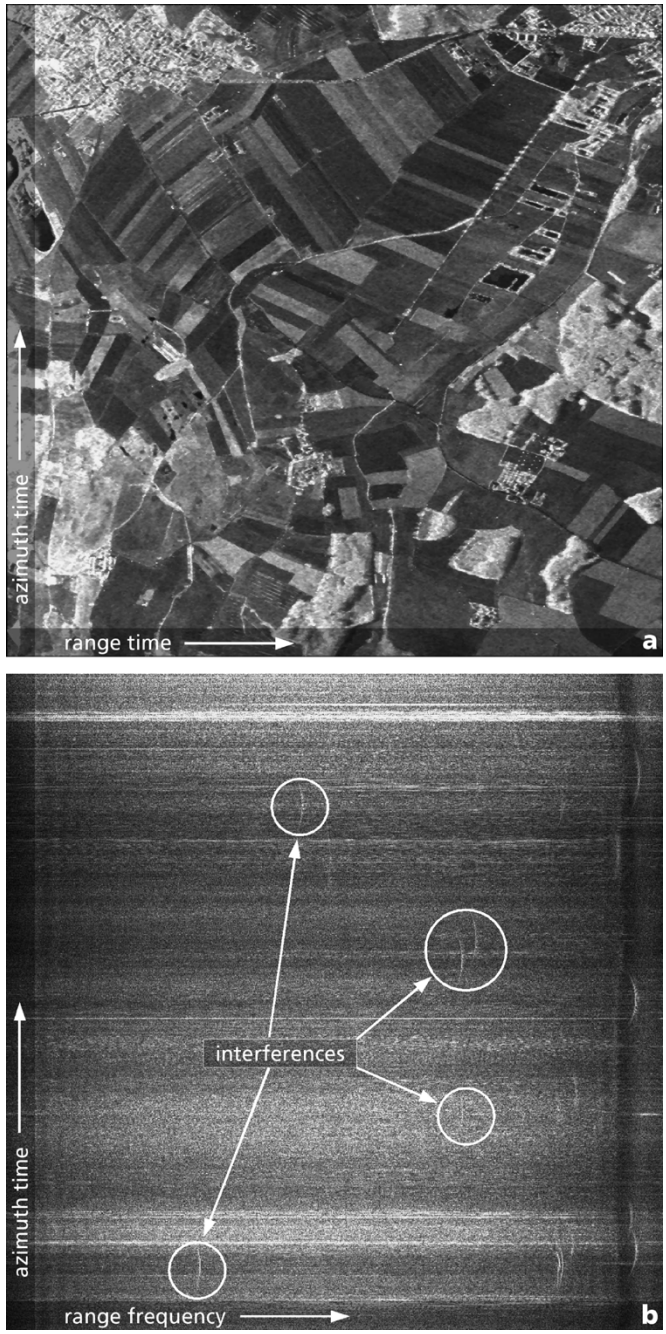

Fig. 1. (a) Amplitude of an airborne L-band SAR scene, affected by interferences. The image amplitude appears not significantly deteriorated by interference effects. (b) Range-frequency azimuth-time representation of the data. Interferences become visible as small curved features.

The proposed filtering approach starts with a one-dimensional fast Fourier transform (FFT) in azimuth, to transform the data to range-time azimuth-frequency domain. Then, the phase of (1) is multiplied to the data in order to revert the azimuth compression. (1) is dependent on range; therefore, an update for every range distance is necessary. Azimuth spectral weighting has only little effect on the extension of the RFI

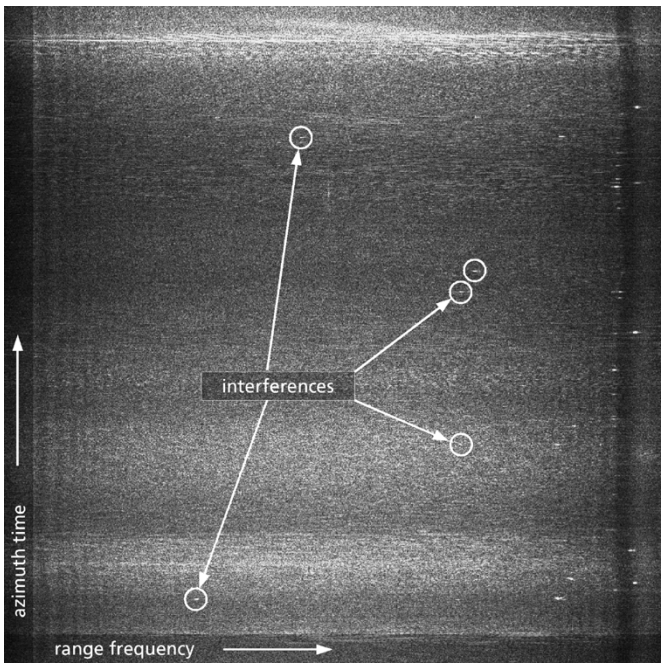

Fig. 2. Range-frequency azimuth-time representation of the L-band SAR scene of Fig. 1, after decompression in azimuth. The interferences are now much better localized in azimuth.

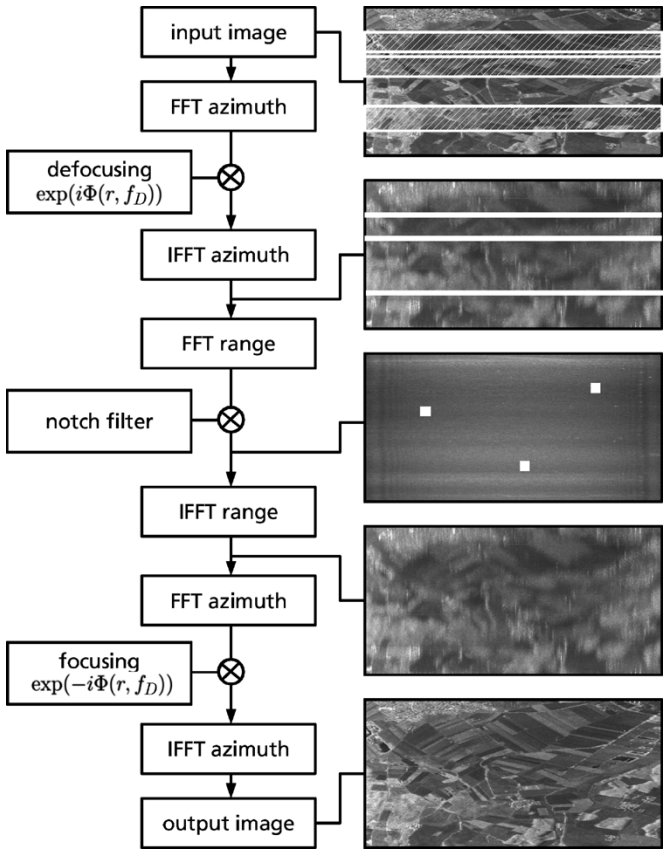

Fig. 3. (Left) Block diagram of the proposed RFI filtering process. The algorithm consists out of a defocusing step according to (1), followed by a notch filter in the range-frequency azimuth-time domain. (Right) Schematic representation of the data and interferences at some processing steps. Interferences are displayed in white (azimuth corresponds to vertical direction).

interferences and can usually be neglected. After an inverse azimuth FFT, interferences appear much better localized in azimuth. Now, a situation similar to that in the case of SAR raw data is reached, and common RFI filtering techniques for SAR raw data can be applied. Fig. 2 shows the example of Fig. 1, after applying the deconvolution step. Instead of curved lines, the interferences appear now as distinct peaks in the range-frequency azimuth-time domain of the data.

A rather simple but common technique for RF interference filtering is to transform the data to the range-frequency domain and to cancel out frequency contributions in every range spectrum with amplitudes higher than a certain threshold [2], [3] (i.e., notch filtering). Other more advanced techniques, originally developed for raw data filtering, may also be used at this stage [7]. If notch-filtering is desired, it is important to choose a filter with a sufficiently large bandwidth so as to entirely remove interference contributions. As described above, the defocusing step does not perfectly revert all processing steps; especially in case of strong range-cell migration, RF interference contributions show a slightly increased bandwidth.

After applying the actual filtering step, the image has to be focused again. This can be achieved by transforming the data back to the range-time azimuth-frequency domain and multiplying by the inverse phase of (1). Finally, an inverse FFT in azimuth leads to the final filtered image. A complete block diagram of the filtering algorithm is shown in Fig. 3.

IV. Experimental Results

The proposed algorithm has been tested on interferometric L-band data, acquired by DLR's experimental SAR system E-SAR in repeat-pass mode over the test site of Alling, Germany. The interferometric baseline of this data acquisition lies between 5–10 m, and the time difference between master and slave image is 14 min. At L-band, E-SAR images have a range bandwidth of 100 MHz and a processed antenna beamwidth of about 7.5°, corresponding to a Doppler bandwidth of about 100 Hz. Typical range distances lie between 3.5–6.5 km. Due to the wide beamwidth at L-band, potential RF interferences become smeared by several hundred meters in azimuth during data processing. Currently, DLR does not perform RF interference filtering at L-band.

This dataset has been used in a study analyzing the varying backscattering behavior of complex targets during the SAR integration time [8]. Depending on the antenna beamwidth in azimuth, targets are illuminated under a set of different look angles, which might cause a nonstationary backscattering behavior. Such a study requires to decompose synthesized SAR images into several azimuthal subapertures with reduced resolution, each corresponding to the scene under different azimuthal look angle.

In the full-resolution image amplitude of the scene [Fig. 1(a)], it is not possible to discern effects caused by RF interferences. However, when subaperture images are formed by splitting the azimuthal spectra into several parts, significant problems with RF interference were encountered. Subaperture images have a reduced SNR, as only small parts of the azimuth response are used for image formation, while sudden RFI remain unmodified.

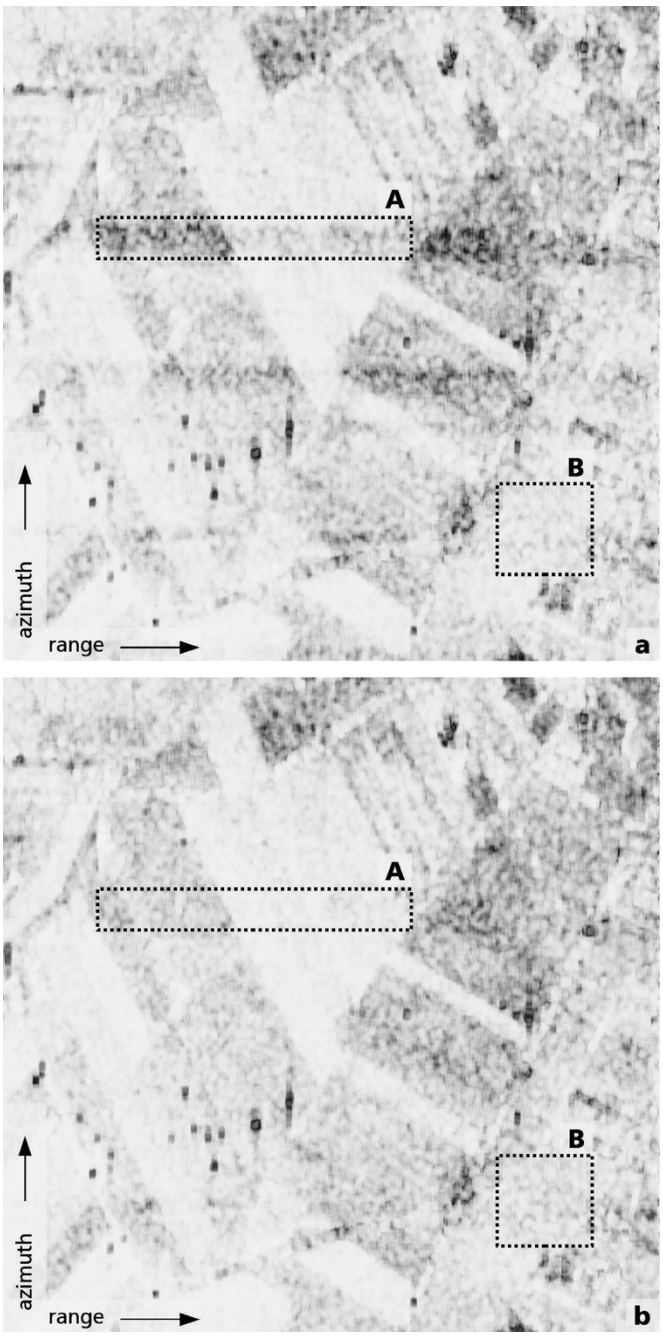

Fig. 4. Interferometric coherence of a 12-Hz subaperture. (a) Before filtering. (b) After applying the proposed filtering method.

Fig. 4(a) shows a coherence map of an interferogram. It has been formed using subaperture versions of the master and slave image with a Doppler bandwidth of 12.5 Hz. Several dark stripes in the range direction, caused by the uncorrelated contributions of different RF interferences in the master and the slave image, are clearly visible. In this example, the interferometric phase itself is influenced by RFI only in form of a noise contribution, which can be analyzed best using the coherence. Stronger interferences may also cause severe phase errors [1], and special care is necessary during filtering to preserve the correct interferometric phase.

Applying the proposed filtering method in both the master and the slave image, an improved coherence map can be obtained [shown in Fig. 4(b)]. Most of the dark stripes with reduced correlation have disappeared. In Table I, coherence estimates for two regions of Fig. 4 are given. Area A represents an area significantly affected by interferences, while area B is almost unaffected.

TABLE I
EFFECT OF RFI FILTERING ON THE INTERFEROMETRIC COHERENCE

Region in Fig. 4	before filtering	after filtering
A	0.809271	0.926450
B	0.941032	0.920849

In the example of Fig. 4, notch-filtering in the range-frequency domain was performed after defocusing of the image. The optimum filter width and threshold value depend on the data and the sensor characteristics themselves. For E-SAR L-band data, it was found that it is sufficient to cancel regions of ± 2 pixels around the peak positions (corresponding to a band rejection of approximately 250 kHz). As a threshold, three times the mean of the average amplitude of the respective line has been used. Of course, the influence of spectral weighting applied during data processing has to be considered in the choice of the threshold values.

It is important to note that different data might require other filtering parameters. The necessary bandwidth of the notch filter is dependent on the amount of range-cell migration in the raw data;[1] at shorter wavelength or lower azimuth resolutions, a narrower notching might be sufficient. Also, the characteristics of the interferences encountered in the data are essential for correctly tuning the filter parameters. The strength of the filter can be adjusted by changing the threshold value: A smaller threshold filters out more and weaker RF interferences. However, a too low threshold value would cause many frequencies to be canceled, which might seriously corrupt the impulse response function.

Generally, this method cannot be expected to yield perfectly filtered images. Apart from a possible incorrect detection of RF interferences, the filtering also cannot be applied symmetrically to master and slave image. As the formation of the interferogram correlates the spectra of the images, the missing spectral components reduce the amplitude of the correlation result, equivalent to a loss of coherence. The expected amount of coherence loss is, therefore, related to the percentage of filtered bandwidth. This effect can be observed in area B of Fig. 4: after filtering, the RF interference effects have almost disappeared, but some areas show a small decrease in coherence (see Table I). However, when the filter parameters are chosen carefully, the gains of this method by far outweigh its disadvantages.

V. CONCLUSION

Image degradation due to RF interferences is an important problem in SAR imaging, which cannot be neglected during advanced SAR image analysis. Among other things, RF interferences might cause, in particular, a significant loss of coherence

[1]About five range-cells for the data used in this study.

in affected regions, even when the image amplitude remains almost undisturbed. Consequently, an operational filtering of RF interferences is indispensable in applications requiring precise coherence estimates or polarimetric descriptors.

In this letter, a new approach for reducing the impact of RF interferences in synthesized SAR images has been presented. Its principle relies on the transformation of synthesized SAR images into a representation, where common raw-data interference filtering methods can be applied. It can be applied as long as the effects of range-cell-migration do not significantly change the range bandwidth of the interferences. This holds at least for azimuth beamwidths of below 10°, i.e., for most current sensors configurations.

The proposed approach allows an *a posteriori* filtering, when interference problems are encountered during data analysis. This is relevant in many cases, as up to now operational RF interference filtering is only done at lower carrier frequencies, like P-band. Additionally, single-look products effectively became a standard, whereas raw-data products cannot be handled easily even by experienced uses.

Nevertheless, raw-data filtering is still the superior approach and should be performed whenever possible. This would also avoid errors in the polarimetric calibration due to a potential misestimation of calibration parameters in RFI affected regions. In the future, it would be desirable to have the choice of ordering unfiltered (i.e., for pure image analysis) or filtered (i.e., for interferometric/polarimetric parameter estimation) image data.

REFERENCES

[1] A. Potsis, A. Reigber, T. Sutor, and K. P. Papathanassiou, "A phase preserving method for RF interference suppression in P-band synthetic aperture radar interferometric data," in *Proc. IGARSS*, 1999, pp. 2655–2657.

[2] R. T. Lord and M. R. Inggs, "Approaches to RF interference suppression for VHF/UHF synthetic aperture radar," in *Proc. COMSIG*, 1998, pp. 95–100.

[3] S. Buckreuss and T. Sutor, "Suppression of interferences in P band SAR data," in *Proc. IRS*, vol. 3, 1998, pp. 1289–1293.

[4] C. Cafforio, C. Prati, and F. Rocca, "SAR data focusing using seismic migration techniques," *IEEE Trans. Aerosp. Electron. Syst.*, vol. 27, no. 2, pp. 194–207, Mar. 1991.

[5] A. Moreira, J. Mittermayer, and R. Scheiber, "Extended chirp scaling algorithm for air- and spaceborne SAR data processing in stripmap and ScanSAR imaging modes," *IEEE Trans. Geosci. Remote Sensing*, vol. 34, no. 5, pp. 1123–1136, Sep. 1996.

[6] R. Bamler, "A comparison of range-Doppler and wavenumber domain SAR focusing algorithms," *IEEE Trans. Geosci. Remote Sensing*, vol. 30, no. 4, pp. 706–713, Jul. 1992.

[7] G. Cazzaniga and A. Monti-Guarnieri, "Removing of RF interferences from P-band airplane SAR data," in *Proc. IGARSS*, 1996, pp. 1845–1847.

[8] L. Ferro-Famil, A. Reigber, and E. Pottier, "Time-frequency analysis of natural scene anisotropic scattering behavior from Pol-In-SAR data," in *Proc. EUSAR*, 2004, pp. 251–254.